Chapter 2
Cosmology Background

The current standard model of the Universe is one which is homogeneous and isotropic (cosmological principle) in which we as observers occupy no privileged vantage point (Copernican principle). This model is described as the Friedmann-Lemaître-Robertson-Walker model (FLRW) and the particular matter-energy densities of roughly 70 % dark energy (Λ), 25 % dark matter (CDM) and 5 % baryonic matter are described as the ΛCDM model. As a sign that the FLRW ΛCDM model has become the current accepted concordance model of cosmology, we see that there are many excellent and comprehensive standard texts describing this model. The content of this background chapter is largely drawn from the following standard texts: [1–5].

This chapter serves to give a brief overview of some of the cosmological background necessary for the research presented in later chapters. The bulk of the research in this thesis is concerned with the extraction of cosmological parameters from the supernovae data, and in that context, it is sufficient to consider the smooth expanding Universe and its distance measures described in Sects. 2.2 and 2.3. However, this thesis also makes use of CMB data sets, and baryon acoustic oscillation (BAO) data sets, which depend on our understanding of the perturbed Universe, hence a brief overview of the inhomogeneous Universe is also included.

2.1 Prelude: An Historical Overview

Since much of the work in this thesis is focussed on investigating the apparent late time acceleration of the expansion of our Universe it seems fitting to include a brief historical note about the first observations which suggested that our Universe is indeed expanding, Einstein's independent suggestion of the cosmological constant, and an early use of standard candles.

In 1929 Edwin Hubble published a paper describing the relationship between the radial velocity and distance of certain extragalactic 'nebulae' [6]. Hubble's methodology for determining distance depended on the knowledge that certain types

M. C. March, *Advanced Statistical Methods for Astrophysical Probes of Cosmology*, Springer Theses, DOI: 10.1007/978-3-642-35060-3_2,

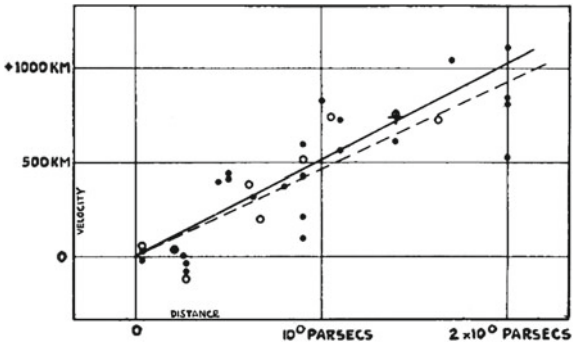

Fig. 2.1 Plot from [6] showing that more distant objects recede more rapidly than nearby objects, a result that challenged the conventional wisdom of the time, suggesting that the universe was not static, but dynamic and expanding

of astrophysical objects within the extragalactic 'nebulae' had a known absolute magnitude, or at the very least had an absolute magnitude which lay within a small, well known range. By observing the apparent magnitude of known types of objects and comparing this to their supposed absolute magnitude, their distances could thus be calculated. Hubble essentially used objects of known brightness (such as Cepheid variables, novae and blue stars) as 'standard candles', that would appear dimmer at greater distances and brighter at closer distances. The velocities of the extra galactic nebulae were obtained from observations of their redshift.

Hubble concluded that a 'roughly linear' relationship existed between the velocities and distances of these extragalactic nebulae, as shown in Fig. 2.1. The velocity, v_{obs}, as observed from Earth, was proportional to the distance, $d(t_0)$, for low redshift $z \lesssim 0.1$, extragalactic objects:

$$v_{\text{obs}} = H_0 d(t_0) + v_{pec} \tag{2.1}$$

where H_0 is the value of the Hubble parameter today and v_{pec} is the peculiar velocity of the object due to local gravitational interactions. The recessional velocity, $v(t_0)$, is defined as:

$$v(t_0) = H_0 d(t_0) \tag{2.2}$$

where subscript 0 denotes values today. On scales larger than 100 Mpc, the universe appears to be both isotropic and homogeneous and the Hubble parameter has no spatial dependence. For scales greater than the scale of homogeneity, the peculiar velocity is small with respect to the recessional velocity and can be neglected. Hubble's observations that the further away an object is, the more rapidly it is receding, confirmed the theoretical predictions of [7] that an expanding universe was indeed a valid solution to Einstein's theory of General Relativity.

Hubble's tentative 1929 result for extragalactic objects at low red shift, has been subsequently confirmed by modern observations. Furthermore, it has been shown that the Hubble parameter varies with higher redshift (or earlier times), such that $H = H(t)$ and:

$$\dot{r}(t) = H(t) r(t) \tag{2.3}$$

where $r(t)$ is the distance in the radial direction and overdots denote derivatives with respect to time, t. The relationship between the physical distance, $r(t)$ and the comoving distance, χ is given by:

$$r(t) = \chi a(t) \tag{2.4}$$

where $a(t)$ is known as the scale factor and the Hubble parameter is defined as:

$$H(t) \equiv \frac{\dot{a}(t)}{a(t)} \tag{2.5}$$

Having defined the Hubble parameter which describes the expansion rate of the universe, it is of interest to know what physical processes control this parameter. As shall be discussed in some detail later, it is Friedmann's equation which describes the physics governing the Hubble Rate:

$$H^2(t) = \left(\frac{\dot{a}(t)}{a(t)}\right) = H_0^2(\rho_m(t) + \rho_r(t) + \rho_\Lambda(t) + \rho_K(t)) \tag{2.6}$$

H_0, is the value of the Hubble Rate today and is a constant, meaning that the time dependent Hubble rate, $H(t)$ is governed entirely by the sum of the evolving energy densities, (i.e. $\rho(t)s$) of the principal constituents of the universe. The equations describing the energy densities due to matter, $\rho_m(t)$ and radiation, $\rho_r(t)$ are well understood and shall be discussed in due course. $\rho_K(t)$ represents the contribution to the energy density due to the curvature of the universe, a term which vanishes in the case of a flat universe. However, it is $\rho_\Lambda(t)$ which is the term of special interest for the research presented in this thesis.

When $\rho_\Lambda(t)$ is considered to be constant, such that $\rho_\Lambda(t) = \rho_{\Lambda_0}$, then it is traditionally termed the 'Cosmological Constant', but when it is allowed to vary with time, it is known as 'Dark Energy'. The form which $\rho_\Lambda(t)$ takes is by no means certain and there are many unanswered questions regarding its nature and origin. Some of the initial questions which this project seeks to answer include identifying whether $\rho_\Lambda(t)$ has evolved with time, whether it is still evolving with time, what values it may take and whether it is the same in all directions.

In order to constrain the form of the dark energy term, $\rho_\Lambda(t)$, it is necessary to map out how $H(t)$ varies in time and discern how this can be affected by the $\rho_\Lambda(t)$ term in Eq. (2.6). Edwin Hubble mapped out the evolution of $H(t)$ using a 'standard candle' technique and a similar methodology is used today with the supernovae type Ia—this is the particular focus of Chap. 7. As well as 'standard candles', 'standard rulers' can be used to map out the expansion history of the Universe. The idea of a standard ruler is to take some object of fixed co-moving length, χ and measure its physical length, $r(t)$ at various known times (i.e. at different redshifts).

No astrophysical objects have been identified as being suitable candidates for standard rulers, but a cosmological phenomenon has been identified as being appropriate: Baryon Acoustic Oscillations. Although in accordance with the cosmological

principle, the universe is isotropic and homogeneous on large scales, it is lumpy on small scales (<100 Mpc). On small scales, matter is clumped into over and under densities which are distributed according to preferred length scales, preferred scales which were established by the physical processes occurring around the time of recombination. The idea is to use these preferred scales in the matter distribution as standard rulers to probe the history of the universe and the evolution or otherwise of the dark energy. Astrophysical observations of galaxies and their spatial distribution reveal the imprint of the baryon acoustic oscillations. Astrophysical observations of this type are used in Chaps. 6 and 8 as probes of cosmology and in particular dark energy.

2.2 The Friedmann Lemaître Robertson Walker Universe

Assuming that the Universe is isotropic and homogeneous, the simplest description of this type of expanding spacetime is give by the Friedman-Lemaître-Robertson-Walker (FLRW) metric; where ds is the spacetime interval. In Cartesian coordinates this is given by:

$$ds^2 = g_{\mu\nu} dx^\mu dx^\nu \tag{2.7}$$

where for an unperturbed universe the FLRW metric is:

$$g_{\mu\nu} = \text{diag}(-1, a^2(t), a^2(t), a^2(t)) \tag{2.8}$$

Transforming into spherical polar coordinates gives another useful form of the FLRW metric, in which the universe can be considered as a 3 dimensional hypersurface embedded in 4-space:

$$ds^2 = -dt^2 + a^2(t)\left[\frac{dr^2}{1 - Kr^2} + r^2 d\Omega^2\right] \tag{2.9}$$

where:

$$d\Omega^2 = d\theta^2 + \sin^2\theta d\phi^2 \tag{2.10}$$

K describes the curvature of the universe:

$$K = \frac{|a|^2}{a^2} \tag{2.11}$$

$$K = \begin{cases} +1 & \text{bounded, positively curved} \\ 0 & \text{unbounded, flat} \\ -1 & \text{unbounded, negatively curved} \end{cases} \tag{2.12}$$

In the case of the curved universe, $K \neq 0$, then the magnitude of the scale factor has geometrical meaning as the radius of curvature of the universe. A further coordinate

transformation allows the FLRW metric to be re written in terms of co-moving distance, χ:

$$ds^2 = -dt^2 + a(t)^2(d\chi^2 + S_K^2(\chi)d\Omega^2) \tag{2.13}$$

where $S_K(\chi)$ is given by:

$$S_K(\chi) = \begin{cases} \sin(\chi) & \text{positively curved} \\ \chi & \text{flat} \\ \sinh(\chi) & \text{negatively curved} \end{cases} \tag{2.14}$$

The relationship between the matter and the gravitational forces (i.e. geometry) of the Universe, are codified in the Einstein equations; which are stated here without proof. For a detailed description see for example [8].

$$G_{\mu\nu} = 8\pi G T_{\mu\nu} \tag{2.15}$$

where the Einstein Tensor is:

$$G_{\mu\nu} = R_{\mu\nu} - \frac{1}{2} g_{\mu\nu}\mathcal{R} \tag{2.16}$$

with and $R_{\mu\nu}$ and $\mathcal{R}$ being the Ricci tensor and scalar respectively:

$$R_{\mu\nu} = \Gamma^{\alpha}_{\mu\nu,\alpha} - \Gamma^{\alpha}_{\mu\alpha,\nu} + \Gamma^{\alpha}_{\beta\alpha}\Gamma^{\beta}_{\mu\nu} - \Gamma^{\alpha}_{\beta\nu}\Gamma^{\beta}_{\mu\alpha} \tag{2.17}$$

$$\mathcal{R} = g^{\mu\nu} R_{\mu\nu} \tag{2.18}$$

The comma notation indicates a partial derivative. $T_{\mu\nu}$ is the stress-energy tensor, which describes the characteristics of the 4-momentum flowing through spacetime at any point. The stress-energy tensor for a perfect fluid of pressure, p and density, ρ, flowing with 4-velocity u^{μ} may be written as:

$$T_{\mu\nu} = (\rho + p)u^{\mu}u^{\nu} + pg^{\mu\nu} \tag{2.19}$$

The right hand side of Einstein's equation quantifies the amount of matter and the left hand side is a statement about the geometry of the spacetime. The Einstein tensor is constructed from the Ricci tensor and scalar. Einstein realized that the initial equation he proposed allowed for a dynamic, expanding universe, which at the time was counter intuitive to him, as a static universe was the favoured model of the day. In order to compensate for this and force the universe described in his equation to be static, Einstein added an additional term, the cosmological constant, Λ:

$$G_{\mu\nu} = R_{\mu\nu} - \frac{1}{2} g_{\mu\nu}\mathcal{R} - g_{\mu\nu}\Lambda \tag{2.20}$$

Einstein originally added his additional term $g_{\mu\nu}\Lambda$ to the left hand side of Eq. (2.20), signifying a modification to gravity, but in modern discussions of the cosmological constant the term is generally subtracted from the right hand side of Eq. (2.20) indicating a modification to the matter-energy content of the Universe. The effect of introducing Λ was to alter the dynamics to prevent the possible expansion or collapse of the universe, but once it became established through Hubble's observations that the universe was indeed expanding, the additional term could be removed. However as modern cosmological observations seem to indicate that the universe is accelerating [9, 10], a fact which cannot be accounted for by ordinary matter and energy densities, recent years have seen a reinstatement of Λ as a means of explaining this acceleration. Whereas Einstein sought to halt the universe with Λ, modern cosmologists are seeking to accelerate the universe with Λ.

For this background description of the ΛCDM Universe, we shall consider the cosmological constant to be in the form of an additional energy density, in the stress energy tensor. Alternative explanations for the apparent late time acceleration of the Universe are discussed in Chap. 3. In order to obtain solutions to the Einstein equation, it is necessary first of all to obtain the metric connections for the Ricci tensor, which may be calculated directly from the metric. The non zero metric connections obtained are as follows; where overdots denote derivatives with respect to time:

$$\Gamma^i_{0j} = \Gamma^i_{j0} = \delta_{ij}\frac{\dot{a}(t)}{a(t)} \tag{2.21}$$

$$\Gamma^0_{ij} = \delta_{ij}a(t)\dot{a}(t) \tag{2.22}$$

Using the metric connections in Eqs. (2.21) and (2.22), with the FLRW metric Eq. (2.8), the Ricci scalar can be calculated via the Ricci tensor to give:

$$\mathcal{R} = 6\left[\frac{\ddot{a}(t)}{a(t)} + \left(\frac{\dot{a}(t)}{a(t)}\right)^2\right] \tag{2.23}$$

Using this to calculate the time, time component of the Einstein equation gives the first Friedmann equation for spatially flat spacetime:

$$H(t)^2 = \left(\frac{\dot{a}(t)}{a(t)}\right)^2 = \frac{8}{3}\pi G\rho(t) \tag{2.24}$$

Calculation of the space, space components of the Einstein equation leads to the second Friedmann equation:

$$\frac{\ddot{a}(t)}{a(t)} = -\frac{4}{3}\pi G(\rho(t) + 3p(t)) \tag{2.25}$$

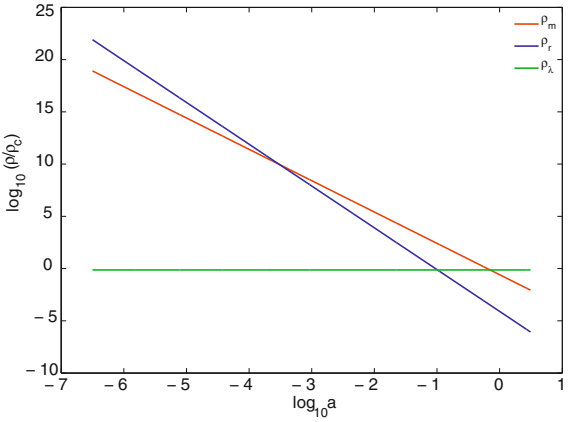

Fig. 2.2 The evolution of energy density with scale factor, shown here for the WMAP best fit parameters (Table 2.1). After the radiation era, the universe passed through matter-radiation equality, and entered the matter dominated era. Matter and radiation densities are diluted as the universe expands, but the relative amount of dark energy or cosmological constant has increased, allowing its density to remain constant or near constant. It is only in the present era that dark energy has begun to dominate the universe

Table 2.1 Summary for WMAP 5 year update best fit parameters for flat ΛCDM model [11]

Description	Symbol	Value
Hubble constant	H_0	71.9 ± 2.7 km/s/Mpc
Baryon density	Ω_b	0.0441 ± 0.0030
Dark matter density	Ω_c	0.214 ± 0.0027
Dark energy density	Ω_Λ	0.742 ± 0.030
Curvature fluctuation amplitude, $k_0 = 0.002$ Mpc^{-1}	$\Delta^2_{\mathcal{R}}$	$(2.41 \pm 0.11) \times 10^{-9}$
Scalar spectral index	n_s	0.963 ± 0.015
Reionization optical depth	τ	0.087 ± 0.017

These two Friedmann equations are of fundamental importance, as they summarise the history of the universe. For a curved universe, the curvature term appears in the Friedmann equation as:

$$H(t)^2 + \frac{K}{a^2(t)} = \left(\frac{\dot{a}(t)}{a(t)}\right)^2 = \frac{8}{3}\pi G\rho(t) \tag{2.26}$$

The pressure $p(t)$ and density $\rho(t)$ terms in Eqs. (2.24) and (2.25) can be expressed as sums of the $p(t)s$ and $\rho(t)s$ of the various fluids that make up the universe, provided that the fluids are non-interacting. The cosmological constant and curvature term may be included as fluids with contributing densities, such that:

$$\rho(t) = \rho_m(t) + \rho_\gamma(t) + \rho_\Lambda(t) + \rho_\kappa(t) \tag{2.27}$$

where:

$$\begin{array}{ll} \rho_m(t) \text{ non relativistic pressureless matter (dust)} & w = 0 \\ \rho_\gamma(t) \text{ relativistic matter (photons)} & w = 1/3 \\ \rho_\Lambda(t) \text{ cosmological constant} & w = -1 \\ \rho_\kappa(t) \text{ curvature} & w = -1/3 \end{array} \tag{2.28}$$

The energy densities can be calculated, using the relativistic continuity equation [1], where w is the equation of state parameter $w = p/\rho$:

$$\frac{\partial \rho}{\partial t} + 3H(t)(\rho + p) = 0 \tag{2.29}$$

which in terms of a is:

$$\frac{\partial \rho}{\partial t} + 3\frac{\dot{a}(t)}{a(t)}(1 + w)\rho = 0 \tag{2.30}$$

which in the case of constant w has solutions of the form below:

$$\rho(t) = \rho_0 a(t)^{-3(1+w)} \tag{2.31}$$

So the Friedmann equation can be written as:

$$H(t)^2 = \left(\frac{\dot{a}(t)}{a(t)}\right)^2 = \frac{8}{3}\pi G(\rho_m^0 a(t)^{-3} + \rho_\gamma^0 a(t)^{-4} + \rho_\Lambda^0 + \rho_\kappa^0 a(t)^{-2}) \tag{2.32}$$

Typically, the densities of the various components of the universe are written in terms of the critical density as cosmological parameters, Ω:

$$\Omega(t) = \frac{\rho(t)}{\rho_c(t)} \tag{2.33}$$

where the critical energy density $\rho_c(t)$ is defined as:

$$\rho_c(t) = \frac{3H^2(t)}{8\pi G} \tag{2.34}$$

In terms of the critical energy density, the Friedmann equation becomes:

$$H(t)^2 = H_0^2(\Omega_m^0 a(t)^{-3} + \Omega_\gamma^0 a(t)^{-4} + \Omega_\Lambda^0 + \Omega_\kappa^0 a(t)^{-2}) \tag{2.35}$$

which also leads to:

$$\Omega_\kappa = 1 - \Omega_{\text{total}} \tag{2.36}$$

where:

$$\Omega_{\text{total}} = \Omega_m + \Omega_\Lambda + \Omega_\gamma \tag{2.37}$$

and

$$\Omega_\kappa = \frac{-K}{a_0^2 H_0^2} \tag{2.38}$$

giving a value for the scale factor today, in a non flat, ($K \neq 0$), universe:

$$a_0^{-1} = \sqrt{|\Omega_{\text{total}} - 1|} H_0 \tag{2.39}$$

The energy density of the dust scales as the inverse volume of the universe, the energy density of the photons also decreases with increase in scale factor, as $\sim a^{-4}$. However, in the model currently under discussion, with $w_\Lambda = -1$ the energy density of the cosmological constant does not vary with time, it is not conserved in the same way as the other quantities—it is not diluted as the universe expands, which means that the relative dominance of the cosmological constant must increase as the universe expands and $\Omega_\Lambda \to 1$.

Our main cosmological interest in the work presented in this thesis is in verifying whether or not this 'cosmological constant' is truly constant with time and whether w_Λ is well constrained to -1. We shall generally use the term 'dark energy' to refer to $\rho_\Lambda(t)$ and reserve the term 'cosmological constant' for models in which $\rho_\Lambda(t) = \rho_{\Lambda_0}$ and $w_\Lambda = -1$. For more details on dark energy models for which $w_\Lambda = -1$ see Chap. 3.

2.3 Cosmological Distance Measures

For our later discussion on the use of standard candles and standard rulers, it is first useful to define a few cosmological distances and measures; for which we generally follow the methodologies of [2] and [1].

2.3.1 Conformal Time

Thus far we have distinguished between physical size of an extended object, $r(t)$ and its comoving size, χ and their relationship via the scale factor:

$$r(t) = \chi a(t)$$

The comoving time, $\eta(t)$, is the maximum comoving distance a photon could have traveled in a given time. Supposing a photon travels a physical distance, dr during a time interval dt, at a velocity, c, in units where $c = 1$, from the metric:

$$dr = dt$$

in comoving coordinates:

$$\frac{d\eta}{dt} = a(t) \tag{2.40}$$

which may be integrated to give the conformal time, $\eta(t)$:

$$\eta(t) \equiv \int_{t_1}^{t_2} \frac{1}{a(t)} dt \tag{2.41}$$

A comoving distance of particular interest is the maximum comoving distance, $\eta_p(t)$ a photon could have traveled since the beginning of the universe:

$$\eta_p(t) = \int_0^t \frac{1}{a(t)} dt \tag{2.42}$$

The comoving distance, $\eta_p(t)$ acts as a boundary which demarcates regions which are causally connected from those which are not causally connected. Any regions which are separated by a comoving distance greater than $\eta_p(t)$ are not causally connected. $\eta(t)$ is known as the 'particle horizon' or 'comoving horizon' and its size increases with the age of the universe.

2.3.2 Redshift and Comoving Distance

The expansion of the universe affects the wavelength of photons in such a way as to be shifted from shorter wavelengths to longer wavelengths, by a measurable amount, known as 'redshift', $z(t)$, which is also a useful measure of distance or time in the universe. This increase in wavelength is indicative of the energy loss of the photon as it does work against the expansion of the universe. Suppose a source at η_e emits a pulse of light of physical duration Δt_e and conformal duration $\Delta\eta$, as shown in Fig. 2.3. The conformal duration is fixed, but the physical duration will vary as the

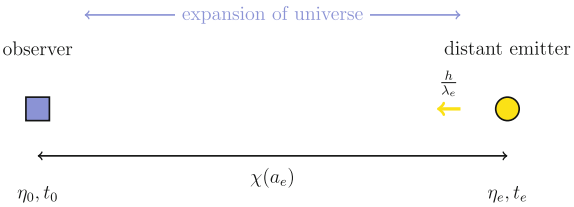

Fig. 2.3 A pulse of light, of wavelength, λ_e, physical duration, Δt_e, conformal duration $\Delta\eta$ is emitted from a distant source, at conformal time, η_e and is received by an observer at conformal time, η_0. χ is the conformal distance, between the observer and the distant emitter

light pulse travels through the expanding universe and will change between the point of emission and the point of observation. At the point of emission, the duration of the pulse is:

$$\Delta t_e = \Delta \eta a(t_e)$$

at the point of observation, the duration of the pulse is:

$$\Delta t_0 = \Delta \eta a(t_0)$$

and as the conformal period is invariant:

$$\frac{\Delta t_e}{a(t_e)} = \frac{\Delta t_0}{a(t_0)}$$

The time interval of the pulse, Δt can be considered to be the time period of the photon, such that $\Delta t = c\lambda$, with $c = 1$ to give:

$$\frac{\lambda_0}{\lambda_e} = \frac{a(t_0)}{a(t_e} \tag{2.43}$$

As can be seen from Eq. (2.43), the wavelength of the photon on arrival at the observer today, λ_0 is longer its wavelength on emission from the source, λ_e, some time in the past. The photon's wavelength has been shifted towards the red end of the spectrum. The 'cosmological redshift', z is defined as the fractional shift in wavelength:

$$z \equiv \frac{\lambda_0 - \lambda_e}{\lambda_e} \tag{2.44}$$

such that:

$$\frac{a_e}{a_0} = \frac{1}{(1+z)} \tag{2.45}$$

It is also useful to have an expression for the comoving distance from the observer out to the distant emitter, labeled $\chi(a_e)$ in Fig. 2.3. This comoving distance can be obtained from Eq. (2.41), but instead of integrating from the beginning of time to the present day, the limits need to be changed to find the the conformal time between the time of emission of the light pulse, t_e, z and time of its observation t_0, $z = 0$. It is also convenient to change to the coordinate of integration to z, such that the comoving distance out to an object at redshift z is:

$$\chi(z) = \frac{1}{a_0} \int_0^z \frac{1}{H(z)} dz' \tag{2.46}$$

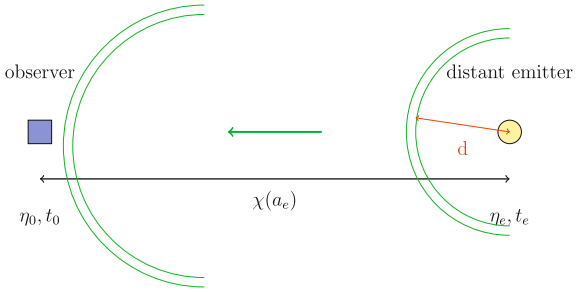

Fig. 2.4 A distant source, of luminosity, L, emits photons in a thin spherical shell, of comoving thickness $\Delta\chi \equiv \Delta\eta$ and physical radius d, which travels out towards the observer

2.3.3 Luminosity Distance

In a generic non-expanding spacetime, the observed flux, F, a distance, d from a far away object of intrinsic luminosity, L is given by:

$$F = \frac{L}{4\pi d^2}$$

Where the luminosity is the total energy, E per unit time, t. To calculate flux in an expanding universe, it is necessary to switch to comoving coordinates, as shown in Fig. 2.4 and consider the path of a thin shell of photons, of comoving thickness $\Delta\chi \equiv \Delta\eta$ and physical duration Δt, emitted from the distant source at η_e. The energy emitted by the source is given by:

$$\Delta E(t_e) = L\Delta t_e \tag{2.47}$$

which in comoving coordinates is:

$$\Delta E(\eta_e) = La(\eta_e)\Delta\eta \tag{2.48}$$

The energy of a single photon is $E = 1/\lambda$, as the photons in the thin spherical shell move through the expanding universe, they are redshifted and loose energy, as described in Eq. (2.43), such that the energy of each observed photon is $E_0 = E_e\frac{a_e}{a_0}$. This means that there is an overall decrease in the energy contained in the thin shell by the time it reaches the observer:

$$\Delta E(\eta_0) = L\frac{a(\eta_e)^2}{a(\eta_0)}\Delta\eta \tag{2.49}$$

On reaching the observer, the physical surface area, $A(\eta_0)$ of the shell is:

$$A(\eta_0) = 4\pi\chi(a_e)^2 a(\eta_0)^2 \tag{2.50}$$

and its physical duration is:

$$\Delta t(\eta_0) = a(\eta_0)\Delta\eta \tag{2.51}$$

Thus in a flat expanding universe, the flux, i.e the energy per unit area per unit time, at the observer is given by:

$$F(\eta_0) = \frac{L}{a_0^2 4\pi\,\chi_e^2(1+z)^2} \tag{2.52}$$

where the comoving distance out to the object, $\chi_e \equiv \chi(a_e)$ is given by Eq. (2.46) in the general case of a curved universe, the flux is:

$$F(\eta_0) = \frac{L}{a_0^2 4\pi\,S_\kappa(\chi_e)^2(1+z)^2} \tag{2.53}$$

Where $S_\kappa(\chi_e)$ is given by Eq. (2.14) and a_0 is given by Eq. (2.39). The flux received by the observer can be measured, which is usually recorded in terms of the astronomical units of apparent bolometric magnitude, m_{bol}:

$$m_{bol}(z) = -2.5\log_{10} F(z) \tag{2.54}$$

which for an expanding universe is:

$$m_{bol}(z) = 5\log_{10}(S_\kappa(\chi_e)(1+z)) + \text{constant} \tag{2.55}$$

The distance modulus, μ_{bol} is the difference between the intrinsic magnitude of an object, M_{bol} and the observed magnitude of an object:

$$\mu_{bol} = m_{bol} - M_{bol} \tag{2.56}$$

The luminosity distance, d_L, is formally defined as:

$$d_L \equiv \left(\frac{L}{4\pi F}\right)^{1/2} \tag{2.57}$$

substituting Eq. (2.52) into Eq. (2.57), gives, for a flat universe:

$$d_L = (1+z)\int_0^z \frac{1}{H(z)}dz \tag{2.58}$$

The distance modulus can be written in terms of the luminosity distance:

$$\mu = 5\log\left[\frac{c}{H_0}\frac{d_L}{1\,\text{Mpc}}\right] + 25 \tag{2.59}$$

This is the key equation for probing the expansion history of the universe using so-called standard candles. For a class of objects of fixed intrinsic magnitude, distributed over various redshifts, the distance modulus can be predicted for a given cosmology and compared with observed measurements to identify which cosmological model gives the best description of the observed universe.

2.3.4 Angular Diameter Distance

If a distant object at redshift, z, of known physical length, l, is subtended by an angle, θ, as in Fig. 2.5, then the distance, d_A out to that object is the angular diameter distance; which in physical coordinates is:

$$\theta = \frac{l}{d_A} \tag{2.60}$$

or in comoving coordiantes:

$$\theta = \frac{l}{a_e} \frac{1}{\chi(a_e)} \tag{2.61}$$

Equating Eqs. (2.60) and (2.61) gives an expression for the angular diameter distance in a flat universe:

$$d_A = a_e \chi(a_e) = \frac{\chi(z)}{(1+z)} \tag{2.62}$$

where the comoving distance out to the object, $\chi(a_e)$ is given by Eq. (2.46). It can also be useful to write the luminosity distance in terms of the angular diameter distance in this way:

$$d_L = (1+z)^2 d_A \tag{2.63}$$

where the scale factor today is unity $a_0 = 1$.

2.4 Inflation

The theory of inflation was devised primarily by [12, 13] in the early 1980s as a means of explaining several cosmological problems, which were yet unexplained by the standard big bang model. A very brief overview of inflation is included here, partly because of its role in the description of the initial inhomogeneities and partly because there are some similarities between the mechanisms which drove inflation and some of the ideas used to describe dark energy. The similarities arise because both inflation and dark energy deal with the case of an accelerating universe; the acceleration during inflation was much more extreme than the slow acceleration seen today, however, the two scenarios share some common ground.

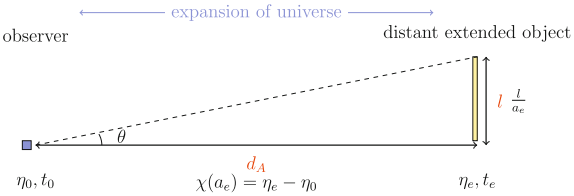

Fig. 2.5 Angular diameter distance, d_A: a distant extended object of physical length, l, subtends an angle θ on the sky. Physical dimensions are shown in *red*; comoving distances and coordinates are shown in *black*; θ is the same in both comoving and physical dimensions

The main problems which inflation sought to solve were the so-called flatness and horizon problems. The distribution of the photons released at recombination and observed today initially by Penzias and Wilson and later by space borne instruments such as COBE and WMAP, was seen to be inhomogeneous on small scales, but statistically homogeneous on large scales, $\theta \gtrsim 1°$. The problem is why do regions that would not have been not causally connected at recombination (when the CMB was released) appear to be statistically statistically homogeneous today? According to inflation, this problem can be solved if the universe undergoes a brief period of rapid expansion at early times.
The expression for the comoving horizon, Eq. (2.41) may be re-written as:

$$\eta(a) = \int_0^a \frac{1}{aH(a)} \frac{da}{a} \tag{2.64}$$

where the comoving Hubble radius is defined as:

$$\frac{1}{aH(a)}$$

The comoving horizon separates regions which are currently causally separated and have been causally separated since all time. The comoving Hubble radius separates regions which are currently causally separated, but may have been causally connected in the past [1]. If the Hubble radius is smaller than the comoving horizon, then regions which are today separated by the Hubble radius, but lie within the comoving horizon, could have been causally connected in the past, even though they are causally disconnected.
In order to have a decreasing Hubble radius, $aH(a)$ must be increasing:

$$\frac{d}{dt}\left(\frac{a}{a}\frac{da}{dt}\right) > 0$$

such that we have an accelerating universe:

$$\frac{d^2a}{dt^2} > 0 \tag{2.65}$$

Our main interest here is to discern what drives this acceleration. Substituting Eq. (2.65) into the second Friedmann equation, Eq. (2.25) tells us something about the energy density involved:

$$0 < -\frac{4}{3}\pi G \underbrace{(\rho(t) + 3P(t))}_{\text{must be negative}} \tag{2.66}$$

$$P(t) < -\frac{\rho(t)}{3} \tag{2.67}$$

which demands that the pressure, $P(t)$ is negative, as the energy density, $\rho(t)$ is positive. This describes something completely different from ordinary matter and radiation, which always has a positive pressure. Guth identified this negative pressure as the driving force behind the exponential expansion [12] and this negative pressure could, for example, be supplied by a scalar field with a Lagrangian:

$$\mathcal{L} = \frac{1}{2} g^{\mu\nu} \partial_\mu \phi \partial_{nu} \phi - V(\phi) \tag{2.68}$$

which has a stress-energy tensor:

$$T^{\mu\nu} = \frac{1}{2}\dot{\phi}^2 - \frac{1}{2}(\nabla\phi)^2 - g^{\mu\nu} V(\phi) \tag{2.69}$$

whose time–time component gives the energy density:

$$\rho = \frac{1}{2}\dot{\phi}^2 + V(\phi) \tag{2.70}$$

and whose spatial components give the pressure:

$$P = \underbrace{\frac{1}{2}\left(\frac{\partial\phi}{\partial t}\right)^2}_{\text{kinetic term}} - \underbrace{V(\phi)}_{\text{potential term}} \tag{2.71}$$

In order for P to be negative, then the potential energy must be greater than the kinetic energy. Guth's original idea for such a scenario was to have a field trapped in a false minimum; because the field was trapped, it would have little kinetic energy and because it was in a false minimum, the potential energy could be a suitable non-zero value. The problem with Guth's original idea was how a 'graceful exit' could be made from entrapment in the false minimum, bringing the epoch of inflation to an end.

Linde [13] reviewed some of the various modifications to Guth's 'old' inflationary theory and developed a 'new' inflationary model in which the field was not trapped in a false minimum, but began at some positive potential from which it could freely and

slowly 'roll' towards the true vacuum potential. As well as solving the problem of escape from the false minimum, Linde's new model also had the added and important benefit of predicting that the density perturbations produced during the slow roll inflation are inversely proportional to $\dot{\phi}$ [14], such that the over-densities, $\delta\rho$ for different momenta, k are given by [13]:

$$\frac{\delta\rho(k)}{\rho} = \frac{1}{\sqrt{2}\pi^3}\frac{H^2}{|\dot{\phi}|}\bigg|_{\phi=\phi^*} \tag{2.72}$$

where ϕ^* is the value of the field at the moment at which the momentum k of this perturbation was equal to $k_* = H$. The end of inflation occurs when the field finally reaches the true minimum and oscillates about that minimum for some time before decaying and producing elementary particles as it decays. Thus ends our brief and highly simplified description of inflation. The so-called 'new' inflation that we have outlined serves to illustrate the main principles of inflation, however, there are other inflationary theories offering refinements and developments. Some of these developed theories include 'chaotic inflation', which does not assume thermal equilibrium for its initial conditions and 'hybrid inflation' which uses multiple scalar fields.

2.5 The Evolution of the Inhomogeneities

One of the useful outcomes of the inflation model is that it predicts the initial distribution of density inhomogeneities, in Eq. (2.72), which eventually give rise to the large scale structure of the present day universe and the temperature anisotropies in the CMB. The power spectrum of these initial over and under densities is usually parametrized in the following way, (e.g. [15]) and is termed the 'primordial power spectrum':

$$P_\chi(k) = A_s\left(\frac{k}{k_{s0}}\right)^{n_s-1} \tag{2.73}$$

The power spectrum amplitude, A_s, determines the variance of the fluctuations. The potential of the inflation field determines the spectral index, n_s, with $n_s = 1$ corresponding to the scale invariant power spectrum or Harrison-Zel'dovich-Peebles spectrum. In the slow roll models, where the field is rolling towards the true vacuum, n_s varies very slowly such that $|n_s - 1| \ll 1$.

Having now defined the primordial power spectrum, we wish to know what changes the matter density distribution undergoes in order to produce the present day matter power spectrum and the CMB power spectrum.

The principal constituents of the early universe were photons, baryons and dark matter. Protons and electrons were tightly coupled due to Coulomb scattering and since the mass of the protons is much greater than the mass of the electrons, electrons

are included under the title of 'baryons'. Neutrinos were also present, but we shall omit them from our current discussion.

At early times, the photons and baryons were tightly coupled by Compton scattering into a photon-baryon fluid. Oscillations were set up in this fluid, driven by perturbations in the density distribution of dark matter: the mass of the baryons meant that the fluid tended to fall into the gravitational potential wells in dark matter over dense regions and the radiation pressure of the photons would tend to force the fluid out of the gravitational potential wells. Hence acoustic waves were set up within the photon-baryon fluid with areas of compression having an over density of baryons and areas of rarefaction having an under density of baryons; as long as the photons and baryons were coupled, the fluid continued to oscillate, at characteristic wavelengths related to the speed of sound in the photon-baryon fluid.

Near the time of recombination, the photon-baryon fluid decoupled and the oscillations ceased; baryon over-densities and under-densities were 'frozen in' on a characteristic scale determined by the wavelength of the acoustic oscillations. Decoupled from the baryons, the photons are then free to travel or 'free stream' from the place which they were last scattered, through the universe to be observed today. The surface which connects all the points from which a photon last scattered is known as the last scattering surface or LSS, these photons which were released at the LSS and are observed by us today make up the cosmic microwave background radiation, or CMB. After recombination, the baryons and dark matter continued to interact gravitationally, giving rise to the large scale matter inhomogeneities we see today, and the characteristic matter power spectrum

The physics which governs growth of the inhomogeneities and the behaviour of the photon-baryon fluid is given by perturbation theory, of which a brief overview shall be given. We will give a brief description of the evolution of perturbations in some of the principal constituents of the universe, specifically, we shall look at how photons, baryons and dark matter are distributed and how these distributions change with time. We will also take note of how the perturbations in these affect the metric and how the perturbations in the metric in turn affect the distribution of the photons, baryons and dark matter. We shall not reproduce the full derivation of these perturbations here, (for the full derivation see [1]) however, we shall highlight some of the main ideas involved.

The general strategy is to perturb the metric at first order and then look at how this affects the distribution functions of the various quantities of interest, by looking at how the perturbations to the metric affect the paths of the particles as they move through the universe.

Here, we are considering the growth of perturbations in the early universe, up until the time of recombination. These are the perturbations which are manifested as small inhomogeneities in the CMB, hence we can make linear approximations in this calculation.

For a flat, smooth, expanding universe, spacetime is described by the Friedmann-Robertson-Walker metric; as in Eq. (2.8). In a perturbed universe, small changes in the Newtonian potential, $\Phi(\vec{x}, t)$ and spatial curvature, $\Psi(\vec{x}, t)$, can be introduced to perturb the smooth FLRW metric of Eq. (2.8) in this way:

$$g_{\mu\nu} = \begin{pmatrix} -1-2\Psi(\vec{x},t) & 0 & 0 & 0 \\ 0 & a^2(t)(1+\Phi(\vec{x},t)) & 0 & 0 \\ 0 & 0 & a^2(t)(1+\Phi(\vec{x},t)) & 0 \\ 0 & 0 & 0 & a^2(t)(1+\Phi(\vec{x},t)) \end{pmatrix} \tag{2.74}$$

where the sign convention is such that $\Phi(\vec{x},t) < 0$ and $\Psi(\vec{x},t) > 0$ describe overdense regions, whilst $\Phi(\vec{x},t) > 0$ and $\Psi(\vec{x},t) < 0$ describe underdense regions. One of the key points here is that $\Phi(\vec{x},t)$ and $\Psi(\vec{x},t)$ are small and therefore terms which are quadratic and above in these terms may be dropped. In Eq. (2.74), an explicit choice of gauge has been made, that of the conformal Newtonian gauge. Only scalar perturbations are being considered here.

The distribution function, $f(\vec{x},\vec{p})$ describes the phase space distribution of the various particles;

$$f(\vec{x},\vec{p}) = \frac{1}{e^{(E(p)-\mu)/T} \pm 1} \tag{2.75}$$

(+ for fermions, − for bosons, where $E(p)^2 = m^2 + p^2$, in units where $c = k_B = 1$). The Boltzmann relationship describes how the rate of change in the phase space distribution is related to the collision term $C[f(t)]$ for a given species, it can be expressed as:

$$\frac{df}{dt} = C[f(t)] \tag{2.76}$$

The derivation of the Boltzmann equations looks at how the distribution function for each of the species changes with respect to time in the presence of the perturbed metric. If the species under consideration were non interacting, then the collision term on the right of Eq. (2.76) would be zero; if the species is interacting, then a suitable expression for the interactions must be given, describing the scattering of particles in to and out of the phase space element.

The first order Boltzmann equations we present here are written in Fourier space, in terms of the wave vector, $\bar{k}$ of magnitude k. Primes, ($\prime$), represent differentials with respect to conformal time, η.

2.5.1 Photon and Baryon Perturbations

Photons, protons and electrons are coupled to the metric via gravity and are also coupled to each other. Photons are coupled to electrons through Compton scattering and protons are coupled to electrons through Coulomb scattering; the tight coupling between the the protons and electrons means they share a common over-density, δ_b and a common velocity, v_b.

As the photons travel through the perturbed universe, they gain energy falling into potential wells, lose energy climbing out of potential wells and lose energy overcoming the expansion of the universe. The change in photon energy can be characterized by a change in the photon temperature, δT and we define $\Theta = \frac{\delta T}{T}$, where T is the average photon temperature.

A calculation of the amplitude for Compton scattering provides the collision terms for photon—electron interactions and this scattering affects the direction of the scattered photons. The direction of the photons is given by the momentum direction of the photons, $\hat{p}$ and the relationship between the direction of the photons and the direction of the wave vector is characterized by μ, where $\mu = \frac{\bar{k}.\hat{p}}{k}$. To deal with the directional importance of the photons, the photon perturbations can be described by the $\Theta_l(k, \mu)$ which are expanded in terms of Legendre polynomials, $\mathcal{P}_l$, such that:

$$\Theta_l \equiv \frac{1}{(-i)^l} \int_{-1}^{l} \frac{d\mu}{2} \mathcal{P}_l(\mu)\Theta(\mu) \tag{2.77}$$

$l = 0$ is the monopole $\Theta_0(k)$ which corresponds to the difference between the temperature perturbation at a specific point, and the the average temperature perturbation over all space; $l = 1$ is the dipole $\Theta_1(k)$ which is related to the gradient of the energy density of the photons. Omiting contributions from polarisation, the Boltzmann equation [1] describing photon temperature perturbations is:

$$\Theta' + ik\mu\Theta = -i\Phi' - ik\mu\Psi - \tau' \left[\Theta_0 - \Theta + \mu v_b - \frac{1}{2}\mathcal{P}_2(\mu)\Theta_2 \right] \tag{2.78}$$

which may be expanded using Eq. (2.77). $\tau(\eta)$ is the optical depth and is the distance which a photon may travel on average before being scattered:

$$\tau(\eta) = \int_{\eta}^{\eta_0} a(\eta) n_e \sigma_T \, d\eta' \tag{2.79}$$

where n_e is the number density of the electrons and σ_T is the Thompson scattering cross section. The Boltzmann equations for the baryon perturbations are:

$$\delta_b' + ikv_b = -3\Phi' \tag{2.80}$$

$$v_b' + \frac{a'}{a} v_b = -ik\Psi + \frac{\tau'}{R}[v_b + 3i\Theta_1] \tag{2.81}$$

where the photon to baryon ratio, R, is defined as:

$$\frac{1}{R} \equiv \frac{4\rho_\gamma^{(0)}}{3\rho_b^{(0)}} \tag{2.82}$$

The above equations describe the oscillations of the photon-baryon fluid. Although they seem not to contain an explicit dependence on the dark matter distribution, the dependence on the dark matter is implicit through the dependence on the perturbations to the metric, which are in turn coupled to the perturbations in the dark matter density.

2.5.2 Cold Dark Matter Perturbations

Cold dark matter accounts for some $\sim 25\,\%$ of the energy density of the universe and dominates the matter distribution; it is non-baryonic and interacts only weakly with other particles, but does interact gravitationally. The precise identity of cold dark matter is unknown, but favoured candidates include WIMPs such as the neutralino. The first order Boltzmann equations [1] for cold dark matter with over density, δ and velocity, v are as follows:

$$\delta' + ikv = -3\Phi' \tag{2.83}$$

$$v' + \frac{a'}{a}v = -ik\Psi \tag{2.84}$$

The first order Boltzmann equations, Eqs. (2.78), (2.80) and (2.83) described in this section govern the development of the perturbations in the distributions of photons, baryons and dark matter. In the following sections we shall look at how these equations can be used to explain the inhomogeneities in the large scale distribution of matter today and the anisotropies in the photon distribution of the CMB.

2.6 CMB Angular Power Spectrum

The anisotropies we observe in the CMB today are due to four main factors: Firstly the distribution of photon under densities and over densities at the time of recombination, described by the monopole, $\Theta_0(\eta_\star)$ (where $\eta_\star$ is the conformal time at recombination). Secondly, there are anisotropies due to the perturbations in the gravitational potential at the time of recombination $\Phi(\eta_\star)$; photons released at recombination which were in over dense regions at the time of recombination had to do work to climb out of the gravitational well; photons observed today from over dense regions are less energetic than photons from under dense regions. Thirdly, there is the 'Doppler' effect due to the peculiar velocity of the photons at recombination, as described by the dipole term, $\Theta_1(\eta_\star)$. Fourthly, the effect of a photon falling in to a potential well which is deepening with time causes an overall redshift of that photon.

The effects which are principally responsible for the multiple peak structure in the CMB angular power spectrum are the photon density distribution at recombination, $\Theta_0(\eta_\star)$, and the Doppler effect, $\Theta_1(\eta_\star)$. Since our principal interest in the CMB is the prospect of using the spacing of the acoustic peaks as a standard ruler to probe the expansion history of the universe, we will briefly highlight a few of the necessary steps for obtaining the monopole and dipole terms at recombination, and hence the spacing of the CMB peaks.

We need to obtain suitable expressions for the monopole and dipole from the Boltzmann equation for photons Eq. (2.78). Because we are dealing with the time before recombination, in the tight coupling limit, we can make the approximation that there is no anisotropic stress, such that:

$$\Psi = -\Phi \tag{2.85}$$

and the photon distribution can be completely described by the monopole and dipole terms. Expanding (Eq. 2.78) and retaining only the monopole and dipole terms gives:

$$\Theta_0'(k) + k\Theta_1(k) = -\Phi' \qquad \text{monopole equation} \tag{2.86}$$

$$\Theta_1'(k) + \frac{k}{3}\Theta_0(k) = \frac{k}{3}\Psi + \tau'[\Theta_1 - iv_b] \quad \text{dipole equation} \tag{2.87}$$

Along with the dark matter perturbation equations Eq. (2.83) and baryon perturbation equations Eq. (2.80) there is one other equation we need to describe the evolution of the inhomogeneities: an equation to describe the perturbations in the gravitational potential—for this, we quote without proof [1] the perturbed time–time component of the Einstein equation:

$$k^2\Phi + 3\frac{a'}{a}\left(\Phi' + \frac{a'}{a}\Phi\right) = 4\pi G a^2[\rho_c\delta + 4\rho_r\Theta_0] \tag{2.88}$$

where ρ_c and ρ_r are the dark matter and radiation energy densities respectively.

In theory, there are two main types of initial conditions possible, as set by inflation: adiabatic modes and isocurvature modes. In practice however, observations of the CMB rule out pure isocurvature modes [16], although mixtures of adiabatic and isocurvature modes are possible, [17]. Specific possibilities for isocurvature initial conditions include the baryon isocurvature mode, cold dark matter isocurvature mode, neutrino isocurvature density mode and the neutrino isocurvature velocity mode [18]. Adiabatic initial conditions are those for which there were spatial fluctuations in the total energy density, but not in the entropy, giving initial temperature fluctuations. Isocurvature initial conditions are those for which there were fluctuations in the entropy, but not in the total energy density, leading to near 'isothermal' initial conditions. Here we choose to use adiabatic initial conditions, which for initial time η_i are:

$$\Phi(\eta_i) = 2\Theta_0(\eta_i) \tag{2.89}$$

$$\delta(\eta_i) = 3\Theta_0(\eta_i) \tag{2.90}$$

$$\delta_b(\eta_i) = 3\Theta_0(\eta_i) \tag{2.91}$$

where the initial velocities and monopole are given by:

$$\Theta_1(\eta_i) = \frac{iv_b(\eta_i)}{3} = \frac{iv(\eta_i)}{3} = -\frac{k\Phi(\eta_i)}{6aH} \tag{2.92}$$

In principle, the differential equations for the photon perturbations Eq. (2.86), baryon perturbations Eq. (2.80), dark matter perturbations Eq. (2.83), and gravitational potential Eq. (2.88), can be solved numerically using the adiabatic initial conditions

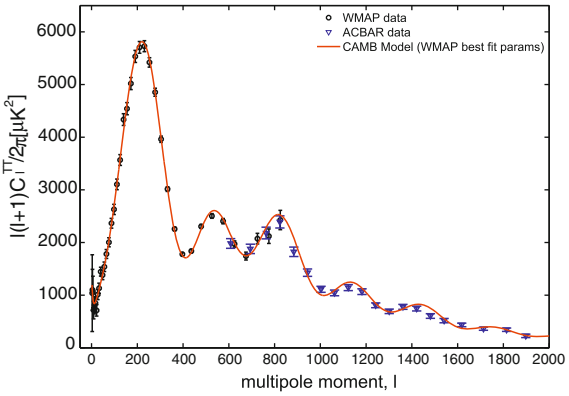

Fig. 2.6 Solid line shows model CMB angular power spectrum produced using CAMB [19] for a ΛCDM model using WMAP best fit parameters (Table 2.1). Data points are from WMAP 5 [20] and ACBAR [21]. The 'acoustic peaks' due to oscillations in the photon-baryon fluid can be seen very clearly from $l = 200$ onwards; these acoustic peaks are also manifest in the galaxy power spectrum. The idea is to use the spacing of these acoustic peaks as a 'standard ruler' for probing the expansion history of the universe

Eq. (2.89), in order to obtain the photon distribution at the time of recombination $\Theta(\eta_\star)$. However, there is also an analytic approach, aspects of which we will briefly highlight here as it gives a physical insight into the physics of the early universe, and the resulting spacing of the CMB peaks.

Hu and Sugiyama [22] developed an analytical method for obtaining the photon density and velocity distribution: From Eq. (2.86), along with the equation for the baryon velocity Eq. (2.80), a second order differential equation can be obtained for the monopole:

$$\Theta_0'' + \frac{a'}{a}\frac{R}{1+R}\Theta_0' + k^2 c_s^2 \Theta_0 = -\frac{k^2}{3}\Psi - \frac{a'}{a}\frac{R}{1+R}\Phi' - \Phi'' \tag{2.93}$$

where the sound speed of the photon-baryon fluid is defined as:

$$c_s \equiv \sqrt{\frac{1}{3(1+R)}} \tag{2.94}$$

Hu and Sugiyama obtained the following monopole solution to Eq. (2.93), for the case of adiabatic initial conditions:

$$\Theta_0(\eta) + \Phi(\eta) = [\Theta_0(0) + \Phi(0)]\cos(k r_s) + \frac{k}{\sqrt{3}}\int_0^\eta d\eta' [\Phi(\eta') - \Psi(\eta')]\sin[k(r_s(\eta) - r_s(\eta'))] \tag{2.95}$$

where $r_s(\eta)$ is the sound horizon, i.e. the comoving distance traveled by a sound wave in conformal time η, and is defined as:

$$r_s(\eta) \equiv \int_0^{\eta} d\eta' c_s(\eta') \tag{2.96}$$

Differentiating Eq. (2.95) gives an expression for the dipole:

$$\Theta_1(\eta) = \frac{1}{\sqrt{3}}[\Theta_0(0) + \Phi(0)]\sin(kr_s) - \frac{k}{\sqrt{3}}\int_0^{\eta} d\eta'[\Phi(\eta') - \Psi(\eta')]\cos[k(r_s(\eta) - r_s(\eta'))] \tag{2.97}$$

The physical insight we gain here is that at recombination the locations of the peaks in the monopole are related to the cosine of the sound horizon, and the locations of the peaks in the dipole are related to the sine of the sound horizon—hence the terminology 'acoustic peaks'. The monopole and dipole terms are out of phase, with the effect that the peaks in the dipole serve to 'fill in' the troughs of the monopole to some extent.

Equations (2.95) and (2.97) go most of the way to describing the photon perturbation at the time of recombination, but to completely describe the photon distribution at the time of recombination, an additional term must be added to describe diffusion damping—i.e to account for the fact that even before recombination, the photons did have some freedom to free stream short distances. However, Eqs. (2.95) and (2.97) do accurately predict the location of the 'acoustic peaks' in the CMB angular power spectrum.

Today, we observe the CMB photons coming from all directions on the sky, with temperature:

$$T(\vec{x}, \hat{p}, \eta) = T(\eta)[1 + \Theta(\vec{x}, \hat{p}, \eta)] \tag{2.98}$$

Since we are observing the projection of the CMB on to a spherical sky, we generally expand $\Theta(\vec{x}, \hat{p}, \eta)$ in terms of spherical harmonics:

$$\Theta(\vec{x}, \hat{p}, \eta) = \sum_{l=1}^{\infty}\sum_{m=-l}^{l} a_{lm}(\vec{x}, \eta)Y_{lm}(\hat{p}) \tag{2.99}$$

where $Y_{lm}(\hat{p})$ are the spherical harmonics and $a_{lm}(\vec{x}, \eta)$ are the observables given by:

$$a_{lm}(\vec{x}, \eta) = \int \frac{d^3k}{(2\pi)^3} e^{i\vec{k}.\vec{x}} \int d\Omega Y^*_{lm}(\hat{p})\Theta(\vec{x}, \hat{p}, \eta) \tag{2.100}$$

The quantity of interest is the angular power spectrum, C_l which is the variance of the $a_{lm}(\vec{x}, \eta)$:

$$\langle a_{lm} a^*_{l'm'} \rangle = \delta_{ll'} \delta_{mm'} C_l \tag{2.101}$$

The observed angular power spectrum for the CMB, as measured by WMAP [20] and ACBAR [21] is shown in Fig. 2.6, along with the ΛCDM model for the WMAP best fit parameters (Table 2.1). The 'acoustic peaks' due to the oscillations in the photon-baryon fluid can be clearly seen from $l = 200$ onwards—these same peaks show up as 'baryonic wiggles' in the matter power spectrum. The idea is to use the spacing of the peaks manifest in the CMB angular power spectrum and the galaxy power spectrum as a 'standard ruler' to probe the expansion history of the universe and constrain dark energy.

The CMB data alone do not constrain dark energy, since dark energy only began to dominate at late times (see for example Fig. 2.2), however, the CMB data can be used in conjunction with other astrophysical probes of cosmology to place tighter constraints on the cosmological parameters. The full CMB data set and likelihood is used directly in our work on Bayesian doubt in Sect. 6.3.2. In the work on cosmological parameter inference from the SNe Ia data, the cosmological constraints are combined with the effective constraints from the CMB. Wang and Mukherjee [23] have shown that the information from the CMB observations relevant to dark energy constraints in the case of a redshift independent dark energy equation of state can be summarised by the CMB shift parameters:

$$R \equiv \sqrt{\Omega_m H_0^2} r(z_{CMB}) \tag{2.102}$$

$$l_A \equiv \pi \frac{r(z_{CMB})}{r_s(z_{CMB})} \tag{2.103}$$

where $r_s(z_{CMB})$ is the comoving sound horizon at recombination as in Eq. (2.96), and $r(z_{CMB})$ is the comoving distance to the recombination surface, where the comoving distance to redshift surface z is given by:

$$r(z) = \frac{c}{H_0} |\Omega_\kappa|^{-1/2} \text{sinn} \left[|\Omega_\kappa|^{1/2} \int_0^z \frac{H_0}{H(z)} \, \text{dz} \right] \tag{2.104}$$

Following [24] we use the R shift parameter to include the constraints from the CMB from the WMAP-5 data [25] in this way:

$$\chi^2_{CMB} = \left[\frac{R(z_{CMB}; w, \Omega_m, \Omega_\Lambda) - 1.710}{0.019} \right]^2 \tag{2.105}$$

Inclusion of the CMB constraints in this way are described in Sect. 7.8 and the confidence intervals produced can be seen in Fig. 7.17.

2.7 Matter Power Spectrum and Baryon Acoustic Oscillations

The distribution of dark matter may be inferred by making observations of galaxies which trace the underlying distribution of dark matter. From these observations, the galaxy (or dark matter) power spectrum can be obtained, which is the Fourier transform of the correlation function and is the matter analogue of the CMB angular power spectrum. The dark matter power spectrum is defined as:

$$P(k) = \langle \delta(\vec{k}) \delta^{\star}(\vec{k}') \rangle \tag{2.106}$$

The acoustic oscillations described in the previous section should show up in the matter power spectrum in a similar way, albeit less pronounced, to the acoustic peaks in the CMB angular power spectrum. The matter power spectrum at late times is given by:

$$P(k, a) = P_{\chi}(k) T(k)^2 \left(\frac{D_1(a)}{D_1(a=1)} \right)^2 \tag{2.107}$$

where $P_{\chi}(k)$ is the primordial power spectrum described by Eq. (2.73) and where the transfer and growth functions, $T(k)$ and $D_1(a)$ are defined as:

$$T(k) \equiv \frac{\Phi(k, a_{late})}{\Phi_{\text{large scale}}(k, a_{late})} \tag{2.108}$$

(for $a > a_{late}$)

$$\frac{D_1(a)}{a} \equiv \frac{\Phi(a)}{\Phi(a_{late})} \tag{2.109}$$

In the regime where the linear approximations are valid, a function for the gravitational potential today $\Phi(k, a)$ may be obtained by numerically solving the differential equations for the photon perturbations Eq. (2.86), baryon perturbations Eq. (2.80), dark matter perturbations Eq. (2.83), and gravitational potential Eq. (2.88), using the adiabatic initial conditions Eq. (2.89) described in the previous section.

The description we have outlined above, is based on the the Boltzmann equations and perturbed Einstein equations for which a number of linear approximations were made. Hence following this methodology leads to the linear matter power spectrum. Although the linear power spectrum may give a good approximation on large scales, it is not valid on small scales. Figure 2.7 shows that the linear and non-linear matter power spectra diverge on small scales (large k). To obtain an accurate non-linear matter power spectrum, an alternative method must be used, such as large N-body simulations [26].

The 'baryon acoustic oscillations', steming from the same origin as the acoustic peaks in the CMB angular power spectrum can be seen in Fig. 2.7, they appear as small wiggles to the right of the turnover point. These baryon acoustic oscillations are washed out by non-linear structure growth at high k. However, baryon acoustic

oscillations can still be seen quite distinctly at lower k, well within the regime which is well described by the linear power spectrum. At higher redshifts, the validity of the linear power spectrum extends to higher k.

The location of the peaks of the baryon acoustic oscillations in the matter power spectrum are directly related to the size of the sound horizon at recombination. The empirical relationship between the oscillations in the matter power spectrum, the acoustic peaks in the CMB power spectrum and the sound horizon at recombination is given by [27]:

$$\frac{P(k)}{P_{\text{ref}}} = 1 + Ak \exp\left[-\left(\frac{k}{0.1h\text{Mpc}^{-1}}\right)^{1.4}\right] \sin\left(\frac{2\pi k}{k_A}\right) \tag{2.110}$$

where A is an amplitude fitting parameter and P_{ref} is a smooth reference power spectrum with no baryons. Crucially, k_A is given by $k_A = \frac{2\pi}{r_s}$ where r_s is the sound horizon at recombination given by Eq. (2.96). The idea is that the co-moving separation of the acoustic peaks or acoustic oscillations in Fourier space act as a cosmological standard ruler. The values for k_A were fixed by the physics of the early universe, which is well understood.

In practice, in the work presented in Chap. 7 the BAO constraint is included using the method suggested by [24] based on [28] where the value A which is independent of the dark energy model is defined as:

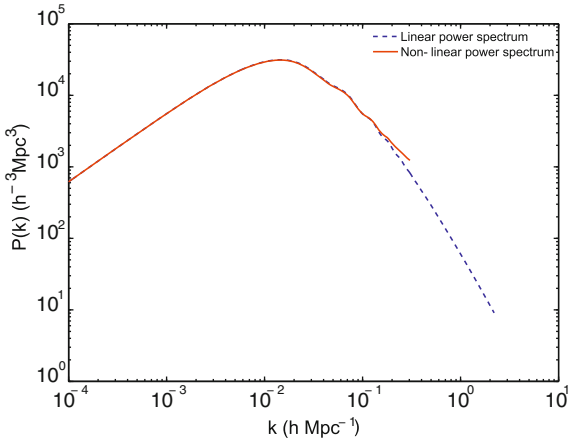

Fig. 2.7 Linear and non-linear matter power spectra produced using CAMB [19] for a ΛCDM model using WMAP best fit parameters (Table 2.1). Calculation of non-linear power spectrum makes use of the HALO fit model [26]. Linear and non-linear power spectra diverge at small scales, where the linear approximations are no longer valid. Baryon acoustic oscillations show up as 'wiggles' in the power spectrum, to the *right* of the turnover from the radiation dominated to matter dominated era

$$A(z_1; w, \Omega_m, \Omega_\Lambda) = \frac{\sqrt{\Omega_m} H_0^{1/3}}{H(z_1)^{1/3}} \left[\frac{1}{z_1 \sqrt{|\Omega_\kappa|}} \text{sinn} \left(|\Omega_\kappa|^{1/2} \int_0^{z_1} \frac{H_0}{H(z)} \text{dz} \right) \right]^{2/3} \tag{2.111}$$

The SDSS LRG constraint can be included in the parameter inference analysis in the following way:

$$\chi^2_{BAO} = \left[\frac{(A(z_1; w, \Omega_m, \Omega_\Lambda) - 0.469)}{0.017} \right]^2 \tag{2.112}$$

The inclusion of this constraint from the BAO data is discussed in Sect. 7.8 and the confidence intervals produced can be seen in Fig. 7.17.

References

1. Dodelson, S.: 2003, *Modern cosmology*, Amsterdam (Netherlands): Academic Press
2. Mukhanov, V.: 2005, *Physical foundations of cosmology*, Cambridge University Press
3. Weinberg, S.: 2008, *Cosmology*, Oxford University Press
4. Peacock, J. A.: 1999, *Cosmological Physics*, Cambridge University Press
5. Schneider, P.: 2006, *Extragalactic Astronomy and Cosmology, An Introduction*, Springer
6. Hubble, E.: 1929, *Proceedings of the National Academy of Science***15**, 168
7. Friedmann, A.: 1924, *Zeitschrift fur Physik***21**, 326
8. Misner, C. W., Thorne, K. S., and Wheeler, J. A.: 1973, *Gravitation*, San Francisco: W.H. Freeman and Co.
9. Riess, A. G., Filippenko, A. V., Challis, P., Clocchiatti, A., Diercks, A., Garnavich, P. M., Gilliland, R. L., Hogan, C. J., Jha, S., Krishner, R. P., Leibundgut, B., Phillips, M. M., Reiss, D., Schmidt, B. P., Schommer, R. A., Smith, R. C., Spyromilio, J., Stubbs, C., Suntzeff, N. B., and Tonry, J.: 1998, AJ **116**, 1009
10. Perlmutter, S., Turner, M. S., and White, M.: 1999b, PhysRevLet **83**, 670
11. Dunkley, J., Komatsu, E., Nolta, M. R., Spergel, D. N., Larson, D., Hinshaw, G., Page, L., Bennett, C. L., Gold, B., Jarosik, N., Weiland, J. L., Halpern, M., Hill, R. S., Kogut, A., Limon, M., Meyer, S. S., Tucker, G. S., Wollack, E., and Wright, E. L.: 2009, ApJS **180**, 306
12. Guth, A. H.: 1981, PhysRevD **23**, 347
13. Linde, A. D.: 1984, *Reports on Progress in Physics***47**, 925
14. Linde, A.: 2005, *arXiv:hep-th/050320*
15. Bridle, S. L., Lewis, A. M., Weller, J., and Efstathiou, G.: 2003, MNRAS **342**, L72
16. Väliviita, J., Enqvist, K., Kurki-Suonio, H.: 2001, in R. Durrer, J. Garcia-Bellido, and M. Shaposhnikov (eds.), *Cosmology and Particle Physics,* Vol. 555 of *American Institute of Physics Conference Series,* p. 320
17. Trotta, R., Riazuelo, A., and Durrer, R.: 2001, PhysRevLet **87(23)**, 231301
18. Bucher, M., Moodley, K., and Turok, N.: 2000, PhysRevD **62(8)**, 083508
19. Lewis, A., Challinor, A., and Lasenby, A.: 2000, ApJ **538**, 473
20. Nolta, M. R., Dunkley, J., Hill, R. S., Hinshaw, G., Komatsu, E., Larson, D., Page, L., Spergel, D. N., Bennett, C. L., Gold, B., Jarosik, N., Odegard, N., Weiland, J. L., Wollack, E., Halpern, M., Kogut, A., Limon, M., Meyer, S. S., Tucker, G. S., and Wright, E. L.: 2009, ApJS **180**, 296
21. Reichardt, C. L., Ade, P. A. R., Bock, J. J., Bond, J. R., Brevik, J. A., Contaldi, C. R., Daub, M. D., Dempsey, J. T., Goldstein, J. H., Holzapfel, W. L., Kuo, C. L., Lange, A. E., Lueker, M., Newcomb, M., Peterson, J. B., Ruhl, J., Runyan, M. C., and Staniszewski, Z.: 2008, *arXive:0801.1491*

22. Hu, W., and Sugiyama, N.: 1995, ApJ **444**, 489
23. Wang, Y., and Mukherjee, P.: 2007, PhysRevD **76(10)**, 103533
24. Kessler, R., Becker, A. C., and Cinabro: 2009a, ApJS **185**, 32
25. Komatsu, E., Dunkley, J., Nolta, M. R., Bennett, C. L., Gold, B., Hinshaw, G., Jarosik, N., Larson, D., Limon, M., Page, L., Spergel, D. N., Halpern, M., Hill, R. S., Kogut, A., Meyer, S. S., Tucker, G. S., Weiland, J. L., Wollack, E., and Wright, E. L.: 2009, ApJS **180**, 330
26. Smith, R. E., Peacock, J. A., Jenkins, A., White, S. D. M., Frenk, C. S., Pearce, F. R., Thomas, P. A., Efstathiou, G., and Couchman, H. M. P.: 2003, MNRAS **341**, 1311
27. Blake, C. and Glazebrook, K.: 2003, ApJ **594**, 665
28. Eisenstein, D. J., Zehavi, I., Hogg, D. W., Scoccimarro, R., Blanton, M. R., Nichol, R. C., Scranton, R., Seo, H.-J.,Tegmark, M., Zheng, Z., Anderson, S. F., Annis, J., Bahcall, N., Brinkmann, J., Burles, S., Castander, F. J., Connolly, A., Csabai, I., Doi, M., Fukugita, M., Frieman, J. A., Glazebrook, K., Gunn, J. E., Hendry, J. S., Hennessy, G., Ivezić, Z., Kent, S., Knapp, G. R., Lin, H., Loh, Y.-S., Lupton, R. H., Margon, B., Mckay, T. A., Meiksin, A., Munn, J. A., Pope, A., Richmond, M. W., Schlegel, D., Schneider, D. P., Shimasaku, K., Stoughton, C., Strauss, M. A., SubbaRao, M., Szalay, A. S., Szapudi, I., Tucker, D. L., Yanny, B., and York, D. G.: 2005, ApJ **633**, 560

http://www.springer.com/978-3-642-35059-7

Advanced Statistical Methods for Astrophysical Probes of Cosmology

March, M.C.

2013, XX, 180 p., Hardcover
ISBN: 978-3-642-35059-7